Magnus Effects on Spinning Transonic Finned Missiles

Arnan Seginer*
Technion—Israel Institute of Technology, Haifa, Israel
and
Izhak Rosenwasser†
Israel Aircraft Industries, Ben-Gurion International Airport, Israel

Magnus forces and moments were measured on a basic-finner model spinning in subsonic and transonic flow. Spin was induced by canted fins or by full- or semi-span, outboard and inboard controls. Magnus force and moment reversals were observed. These were caused by Mach number, reduced spin rate, and angle-of-attack variations. Magnus center of pressure was found to be independent of the angle of attack but varied with the Mach number and model configuration or reduced spin rate. A Mach-number dependent fluid-mechanic mechanism is proposed for the Magnus-force reversal phenomenon on finned configurations.

Nomenclature

a = span of control surface
b = span of the model fins
BD = base drag (Fig. 1)
c = chord of the control surface
C_N = yawing (Magnus) moment coefficient relative to model nose tip, N/qSd
C_y = side (Magnus) force coefficient, Y/qS
d = body diameter, also chord and exposed span of fin
f = spin frequency, rps
h = chord of fin ($h=d$)
l = model length, $l=10\,d$
M = free-stream Mach number
N = yawing (Magnus) moment
N_1, N_2 = normal forces on the fins (Fig. 1)
P = reduced spin rate, $2\pi fb/2V$
q = free-stream dynamic pressure
Re_d, Re_l = Reynolds number, Vd/ν and Vl/ν, respectively
S = body cross-section area, $\pi d^2/4$
V = free-stream velocity
x,y,z = Cartesian coordinates
Y = side force (conventional Magnus force is $Y<0$)
α = angle of attack
δ_e = fin cant angle
ν = kinematic viscosity

Introduction

MANY fin-stabilized munitions and projectiles (e.g., free-falling stores, such as aerial bombs or mortar rounds, sounding rockets, air-to-ground rockets and various missiles) are spun intentionally around their longitudinal axis. This is done to average out asymmetries in fin geometry, mass distribution, and thrust misalignment, in order to minimize dispersion. The spinning motion induces yawing and rolling moments and roll-yaw coupling that may result in high angles of attack, catastrophic yaw, roll lock-in or speed-up.[1] The catastrophic yaw and roll lock-in can be overcome by higher roll rates,[2] but these, whether intentional or the result of roll speed-up, can dynamically destabilize the statically stable projectile by causing a "Magnus instability."[3]

The Tricyclic Theory[4-6] has established the importance of the Magnus moment in determining the dynamic stability of a spinning projectile; and the Magnus coefficients have, consequently, been experimentally investigated quite extensively (e.g., Refs. 7,8), especially when it was shown (contrary to prior assumptions) that the dependence of the Magnus coefficients on the angle of attack and spin rate was highly nonlinear.[1,2] The analysis of the experimental data (force measurements and flow visualizations) identified several mechanisms that could generate side forces (in addition to the potential Magnus force) on a spinning body at incidence. Two of those mechanisms were also applicable to bodies of revolution and were concerned with the spin-induced distortion of the boundary layer on the body in the cross-flow plane. The first was the development of asymmetric boundary layers with asymmetric separation points and, consequently, also with an asymmetric wake, all contributing to a lifting aerodynamic cross-section shape[9] (detail A-A in Fig. 1). The second mechanism, which explains the nonlinear dependence of the Magnus force on the angle of attack better, involved the

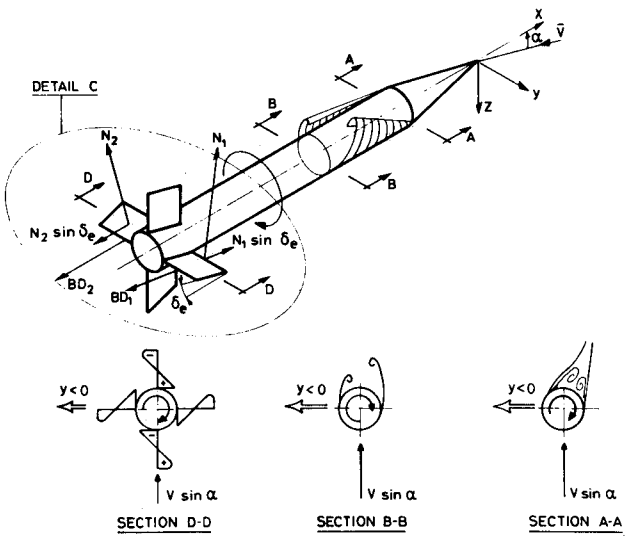

Fig. 1 Mechanism generating Magnus effects on a spinning finned configuration. Detail A-A is the asymmetric boundary layer; detail B-B the asymmetric shed vortices; detail C the asymmetric components of the lift and drag on the fins; detail D-D the leeward fin blanketed by body wake.

Presented as Paper 83-2146 at the AIAA Atmospheric Flight Mechanics Conference, Gatlinburg, TN, Aug. 15-17, 1983; submitted Aug. 22, 1983; revision received Feb. 15, 1985. Copyright © American Institute of Aeronautics and Astronautics, Inc., 1985. All rights reserved.

*Associate Professor, Department of Aeronautical Engineering. Member AIAA.
†Staff Engineer.

vortex pair that was shed from the body. Forced into an asymmetric pattern by the spin-induced circulation, this pair induced a side force on the body[10] (detail B-B in Fig. 1). Both the above mentioned mechanisms exerted side forces in the classic Magnus-force direction, except at low, subcritical Reynolds numbers where the side force reversed its direction.[11]

In addition to the two mechanism acting on the axisymmetric body, three more mechanisms were identified that could induce Magnuslike effects on the spinning fins themselves. The first was a yawing couple, generated by the unequal axial components of the normal forces that acted on the antisymmetrically deflected fins[12] (detail C in Fig. 1). This was the result of the asymmetric angle of attack on opposing fins due to the angle of attack of the whole configuration. This moment was negative relative to the nose tip for positive spin and angle of attack. A second yawing couple was generated by the asymmetric base pressures on opposing fins (detail C in Fig. 1). The third mechanism was more complicated. When the configuration was at an angle of attack and the leeward fin passed through the wake of the body, the aerodynamic force that acted on it was reduced.[7] Because the spin-induced spanwise variation of the aerodynamic load on the fin also changes sign due to the fin deflection (detail D-D, Fig. 1) a negative (classic-Magnus) side force is generated when the root of the fin is immersed in the body wake. The variation of this force with increasing angle of attack is nonlinear, and the force may reverse its direction when the part of the leeward fin that is blanketed by the wake, increases from just an inboard fraction to a major part of the span.[7]

Uselton and Carman[13] mentioned the possibility of an additional Magnus force being produced by an interaction of the asymmetric vortex wake of the body with the leeward fin. Rosenwasser[14] attributed more importance to this mechanism. He pointed out that not only would the leeward fin be affected by the asymmetric vortex wake, but that the trajectories of the vortex cores over the body will be strongly affected by the milling around of the large-span fins, thus, increasing the Magnus effects both on the body and on the fins. This would resemble, although to a much lesser extent, the Magnuslike effects of the wing-tail interference described by Benton.[15]

It was felt that at least some of the above mentioned mechanisms should be Mach-number dependent. However, the bulk of the experimental data on finned projectiles from the above-mentioned investigations was for specific configurations and was either supersonic (intended for use in sounding rocket and missile design) or subsonic (for bombs). The only generally applicable data were those obtained with the Basic Finner configuration,[8] and, of those, the data that were previously acquired at transonic speeds were insufficient for practical engineering design. This investigation was, therefore, undertaken to evaluate the Magnus force and moment on a basic finner spinning in transonic flow. The spinning motion was caused either by canted fins (two cant angles were investigated) or by special, 20%-chord, roll-control surfaces mounted on the uncanted fins. The roll controls included full-span controls as well as half-span inboard or outboard controls. There were three reasons for this choice. It resembled more closely practical configurations and generated a wider range of spin rates. Also, it was hoped that using partial-span control surfaces would furnish additional information on the interactions of the body viscous wake and vortex system with the fins.

Apparatus and Procedure

The investigation was conducted in the 0.5-m by 0.8-m ventilated test section of the induction-type transonic wind tunnel. The model was the basic finner[8] (Fig. 2), with an outer diameter of 45 mm. Two configurations with canted fins ($\delta_e = 7$ and 3 deg, Fig. 2) were tested. Three additional configurations had 20%-chord roll-control surfaces deflected to $\delta_e = 7$ deg (Fig. 3). One had full-span control surfaces (Fig. 3a)

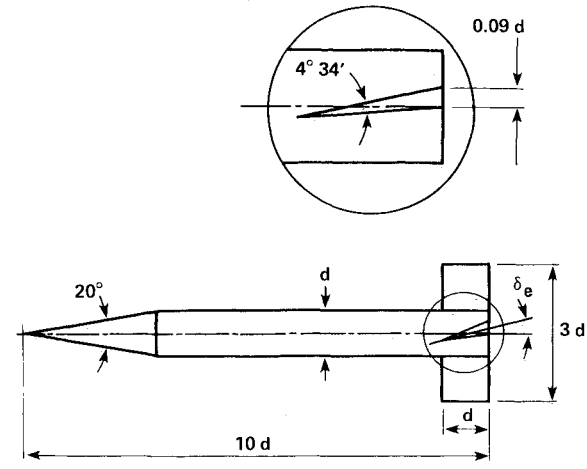

Fig. 2 The Basic Finner with canted fins.

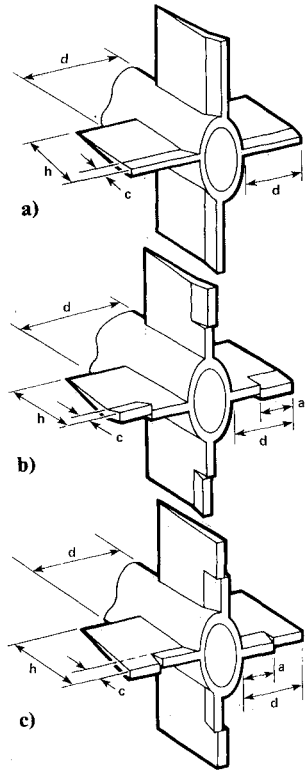

Fig. 3 Configurations of the 20%-chord ($c/h = 0.2$) roll controls. a) Full span, b) outboard semispan ($a/d = 0.5$), and c) inboard semispan.

and the other two had either outboard (Fig. 3b) or inboard (Fig. 3c) half-span controls. The model was mounted on a standard six-component wind-tunnel balance via a bearing-supported free-spinning sleeve. An optical revolution counter, built into the bearing house, measured the spin rate. Details of the system are given in Ref. 16.

The tests were conducted at four Mach numbers, $M = 0.6$, 0.85, 0.95 and 1.1, and the corresponding diameter-based Reynolds numbers were $Re_d = 4.19 \times 10^5$, 5.21×10^5, 5.48×10^5, and 5.73×10^5, respectively. The corresponding length-based Reynolds numbers were $Re_l = 4.19 \times 10^6$, 5.21×10^6, 5.48×10^6, and 5.73×10^6, respectively. At each Mach number, the model was swept through angles of attack from -5 to 15 deg. The output from the balance and revolution counter as well as from the tunnel-parameter transducers was recorded continuously at a rate of 10,000 samples per s. Initially, a pitch-and-pause technique was used, stopping the model at preselected angles of attack and pausing for the spin rate to stabilize. It was found, however, that the spin rate

hardly changed when the angle of attack was varied. This result not only made the testing easier, because the continuous sweep technique could be used, but also indicated that the spin rate (at a given Mach number) depended on the fins' differential angle only and not on the angle of attack.

The output from the revolution counter and the balance was reduced to dimensionless coefficients. The spin frequency f, obtained by integration of the revolution-counter output, was reduced to its commonly used dimensionless form $P=2\pi fb/2V$. The free-stream velocity V was used here rather than the cross flow velocity $V\sin\alpha$ which appeared in another paper[17] dealing with Magnus forces acting on an ogive-cylinder model. It was felt that the mechanisms that were responsible for the Magnus effects on finned projectiles were dominated by the free-stream velocity, whereas the Magnus effects on bodies of revolution could be better correlated by the cross flow velocity.

Forces and moments were reduced to the conventional aerodynamic coefficients using the freestream dynamic pressure and the body cross-section area and body diameter as normalizing area and length, respectively. The moments were computed relative to the model nose tip. The conventional right-hand model coordinate system (Fig. 1) was used. The x axis coincided with the model longitudinal axis, which was also the spin axis, and was positive pointing upstream. The z axis, normal to the x axis, was in the pitch plane and was positive, pointing downward. The y axis was positive, pointing to starboard. With a positive spin (clockwise, facing upstream), as was used throughout this test program, the "classic" Magnus force would be negative, or pointing to port, and the Magnus moment around the nose would be positive. This means that present results with $C_y<0$ have the classic Magnus sense.

All six of the static aerodynamic coefficients were measured at every data point for all the model configurations, including the basic finner with uncanted fins. The latter results compared favorably with similar data from the literature and validated the experimental apparatus and data reduction technique. All the experimental data are presented in Ref. 14. In this article are the data for the Magnus effects only.

Results and Discussion

During the reduction of the data from these experiments, it became apparent that, although the spin frequency for any given configuration almost doubled when the Mach number was increased from $M=0.60$ to $M=1.10$, the reduced spin rate P remained approximately constant (within $\pm 5\%$ for the worst case). This is in agreement with a similar result observed on the completely different configuration of the M823 research store (bomb),[18] although the bomb's spin rate varied somewhat with the angle of attack, while it remained constant for the basic finner (probably due to the different shape of the body especially in the vicinity of the fins). This seems to indicate that the spin frequency f of the basic spinner has the same Mach number dependence as the velocity V, an interesting result in itself.

The independence of the reduced spin rate from the Mach number was observed on all the configurations in the present investigation. The results for any one configuration at all Mach numbers are, therefore, presented on a common plot, emphasizing the Mach-number effect at a constant reduced spin rate.

The side force acting on the model, with fins deflected to $\delta_e=7$ deg, is presented in Fig. 4. Due to the difficulty in measuring the small side forces, the data show some scatter. Curves have, therefore, been hand-faired through the data in order to improve the clarity and readability of the figures. These curves do not necessarily represent accurately the behavior of the data. The same is true of the other figures presenting the side-force and yawing-moment variations.

With fins canted at $\delta_e=7$ deg, the model developed a reduced spin rate of $P\cong 0.17$ at all Mach numbers (Fig. 4). At the two lower Mach numbers $M=0.6$ and 0.85, the Magnus force acted in the classic direction, $C_y<0$ for $\alpha>0$, and the two-side force curves had an almost equal slope around $\alpha=0$ deg. The curves differed only for the higher angles of attack. When the Mach number was increased from 0.85 to 0.95, the Magnus force reversed its sign to positive and increased rapidly when the angle of attack was increased. A further increase in Mach number to $M=1.1$ left the slope at $\alpha\cong 0$ deg approximately unchanged, but for $\alpha\geq 2$ deg the values of C_y increased at a steeper rate than for $M=0.95$. With all other parameters identical for all four curves in Fig. 4, this sign reversal could be attributed to a Mach number effect only. While this effect is not fully understood, the following is an attempt to propose a mechanism that could be its cause.

The asymmetric vortex pair on an axisymmetric body described in detail B-B of Fig. 1, runs downstream, approximately parallel with the body axis in the lateral plane. On a spinning finned body, however, the milling fins induce a circulation on the surrounding flow that must sweep the vortices in the direction of the spin (Fig. 5). A sufficiently high spin rate can deflect the vortices to one side of the fin. Since the strength of the vortex is increasing along the body, that strength reaches its maximum in the vicinity of the fins. The strong vortices would, when deflected to one side of the fin, induce a side force in the direction opposite to the classic Magnus force. This effect should increase with an increasing Mach number because the strength of the vortices is increasing and their trajectories are lower and closer to the fins when the Mach number is higher. With an increasing angle of attack, the vortices move further away from the body and fins and this effect should vanish gradually.

Such an effect could, when sufficiently strong, overcome the other mechanisms that generate the classic Magnus force

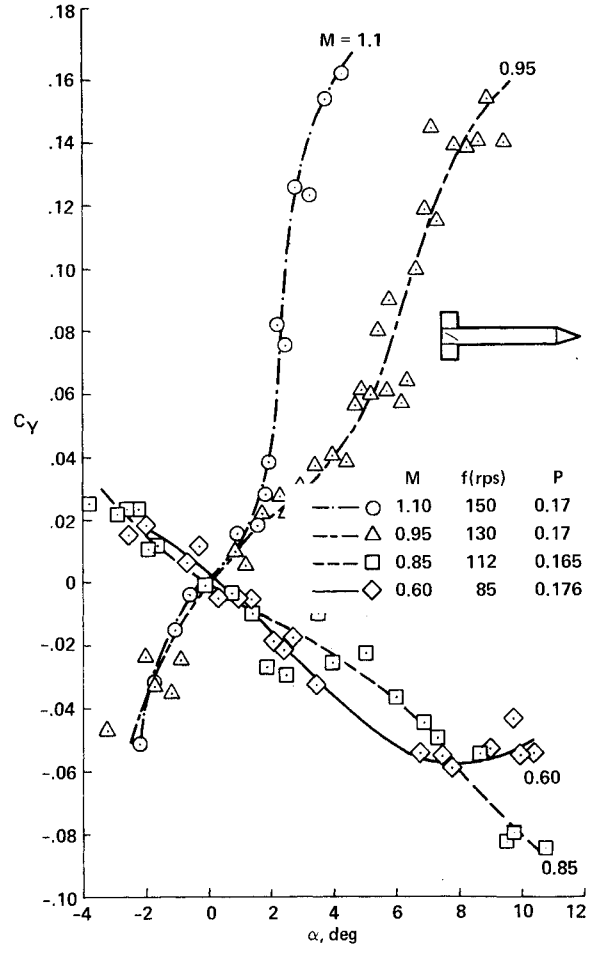

Fig. 4 Side force variation. Full fins deflected, $\delta_e=7$ deg.

and switch the resultant force to the other side. With a weakening of the effect (reduction in Mach number, lower spin rate, higher angle of attack), the other mechanisms should become dominant.

The data in Fig. 4 indicate that the proposed mechanism may be plausible. The side force is switching from negative (classic sense) to positive when the Mach number is increased from $M=0.85$ to $M=0.95$. The switch is quite drastic and may indicate that the vortices moved from above to below the tip of the leeward fin. A further increase in the Mach number increases the side force. This could be the result of the strengthening of the vortices and their still lower trajectories due to the higher Mach number. Note also the highly nonlinear character of the $M=0.95$ and 1.1 curves in Fig. 4 in the vicinity of $\alpha=0$ deg. At very low angles the vortices shed from the body are very weak. At higher values ($\alpha>2$ deg at $M=1.1$ and $\alpha>4$ deg at $M>0.95$), the intensity of the vortices increases significantly and with it also the anticlassic Magnus force. At much higher angles of attack, the vortices may move away from the fin and, therefore, their effect decreases (Fig. 4).

Figure 6 presents the side-force data for the model with fins canted at $\delta_e=3$ deg and a lower reduced spin rate of $P\cong 0.073$. Again, the side force for $M=0.95$ and 1.1 was positive (opposite to the classic Magnus force sense) but had a lower slope than at the higher spin rate of Fig. 4. This could be due to a weaker spin-induced effect on the vortices. On the other hand, the crossover from the negative to the positive values advanced to lower Mach numbers. Although the Magnus force started out as negative (classic) at $\alpha<4$ deg for both $M=0.60$ and 0.85, its slope (again quite similar for both Mach numbers at $\alpha\cong 0$ deg) was lower than with the higher reduced spin rate of Fig. 4 and finally changed from negative to positive. A possible explanation is that at low angles of attack and lower Mach numbers the opposing mechanisms are almost equal in strength. At higher angle of attack ($\alpha>6$ deg), the anticlassic Magnus effect wins with the strengthening of the vortices at $M=0.85$, and the classic mechanism becomes dominant at $M=0.65$ because the weaker vortices move to above the fin tip.

A trend in the Magnus force on finned configurations to change its sign from negative to positive at some transonic Mach number, for a constant reduced spin rate when the angle of attack is increased, as observed in Fig. 6 for $M=0.85$, can also be observed in the data of Refs. 18, 19, and 20. Although the finned configurations in these references differ from the basic finner—some even have freely spinning stabilizers—and although the test conditions (i.e., Mach number, Reynolds number, reduced spin rate, and angle of attack) at which the sign reversal occurs are somewhat different, the resemblance in the general behavior of the data indicates a consistent transonic phenomenon. The dependence of the phenomenon on the configuration and the Reynolds number (see for example, Fig. 4 in Ref. 19) is not surprising in the light of the proposed mechanism. Obviously the span of the fins and the state of the viscous and vortical wake must affect the fin-vortices interaction.

The trend of the Magnus force to reverse its sign at an ever decreasing Mach number as the reduced spin rate is decreasing is continued also in Fig. 7 with the full-span roll-control surfaces. Because of the smaller area of the deflected control surfaces and the resultant lower spin rate, the side force at $M=0.60$ was too small to be measured with sufficient accuracy and is, therefore, not presented. However, the values of C_y at $M=0.85$ that are larger on this configuration than in Fig. 4, clearly indicate an earlier (at a lower Mach number) sign reversal. This trend, also observed in the data of Ref. 18, is consistent with the explanation given above.

Figure 7 also shows a new trend in the data, not observed previously at the higher reduced spin rates. The slope of the Magnus-force curves at $M=1.1$ changed sign and the force coefficient decreased in magnitude quite rapidly for $\alpha>5$ deg.

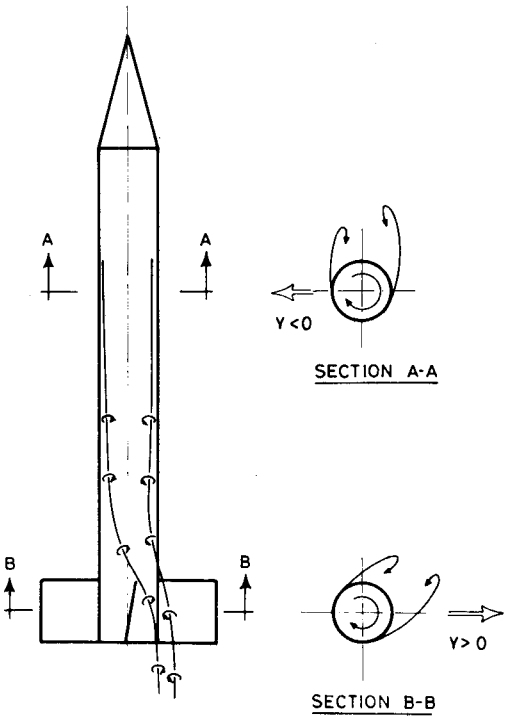

Fig. 5 Vortex trajectories on a spinning finned configuration.

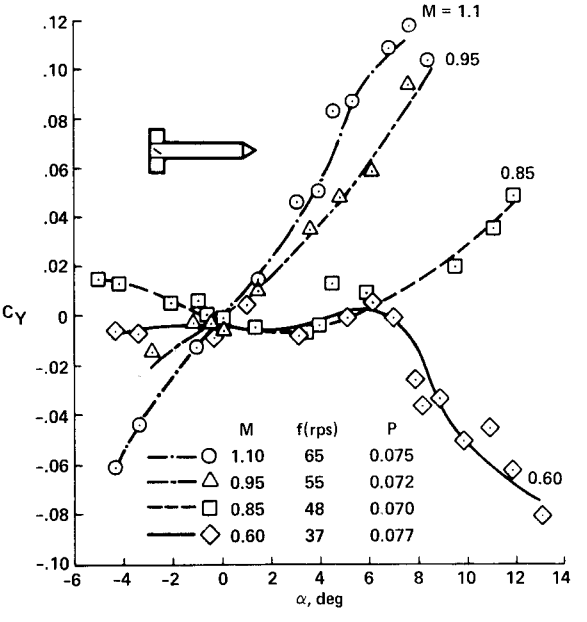

Fig. 6 Side force variation. Full fins deflected, $\delta_e=3$ deg.

The same pattern, a Magnus force that is positive at low angles of attack and turns negative at higher angles, is also repeated at the still lower values of the reduced spin rate ($P=0.01$ and 0.006 for the outboard and inboard semispan roll controls, Figs. 8 and 9 respectively) but this time for both $M=1.1$ and 0.95 (the output at the two lower Mach numbers was too inaccurate to be presented). It is not clear whether the differences between the data in Figs. 8 and 9 are due only to the lower spin rate in Fig. 9 or also to the different location of the roll controls that might have altered the interaction with the body wake and vortices. This pattern is somewhat reminiscent of the positive "bump" in the side force and the "reversed" Magnus force at low reduced spin rates and low angles of attack that were reported by Ref. 21 and 22, respectively.

However, this resemblance may be just fortuitous since the models used in those studies were nonfinned and the tests were conducted at low Mach numbers. A possible explanation of this pattern, based on the displaced-vortices mechanism proposed above, is that with the decreasing spin rate, the displacement of the vortices by the milling fins is decreasing too. Consequently their effect on the fin is felt only at low angles of attack. At higher angles of attack this effect is too weak to balance the classic Magnus effects.

While each of Figs. 4 and 6 through 9 presents the Mach number effects at a constant reduced spin rate, crossplots (not shown here) would emphasize the effects of the reduced spin rate at a constant Mach number. A decrease in the reduced spin rate from 0.17 to 0.016 changes the sign of the side force from negative to positive for the subsonic Mach numbers ($M=0.60$, 0.85). At the same time it reduces the positive values of C_y for the transonic flows ($M=0.95$ and 1.1). At the lowest spin rates the transonic Magnus forces are again negative (in the "classic" direction), except for some positive ("reversed") values at low angles of attack ($\alpha<6$ deg for the outboard roll controls with $P=0.01$, and $\alpha<9$ deg for the inboard roll controls with $P=0.006$). These effects of the spin rate are consistent with the mechanism proposed above.

The Magnus (yawing) moments of the five configurations, corresponding to the Magnus forces of Figs. 4 and 6 through 9, are presented in Figs. 10 through 14. Generally speaking, it can be said that the Magnus-moment curves are very nearly mirror images of the Magnus-force curves. A positive yawing (or classic Magnus) moment correponds to a negative side force (classic Magnus force). Consequently the previous discussion of the side-force curves also applies to the yawing-moment curves once their signs are reversed. When the Magnus force and moment reverse their signs for a given Mach number (e.g., $M=0.8$ in Figs. 6 and 11, or $M=0.95$ and 1.1 in Figs. 8 and 13 and in Figs. 9 and 14), the sign reversals in force and moment do not occur at exactly identical angles of attack. For this to happen, a pure couple has to exist, as was postulated by Regan.[19] This, however, is unreasonable, as the mirror-image resemblance of force and moment implies an approximately constant location of the Magnus center of pressure; whereas, a pure couple would require a sudden discontinuity with the center of pressure going as $x\rightarrow-\infty$ when the Magnus force goes to zero. It is more reasonable to assume that the force and moment do not vanish simultaneously, either because of data scatter, or because of the normal force interaction error that was pointed out by Platou[23] and has not been corrected here.

Finally, since the position of the Magnus center of pressure does not vary with the angle of attack for any one of the combinations of model configurations and Mach number, it was possible to plot (Fig. 15) the position of the center of pressure as a function of Mach number or each configuration. Although the number of data points per configuration in Fig. 15 is insufficient for a description of a continuous, smooth curve, one feature can be deduced from the figure. The Magnus effect on the basic finner has a critical Mach number

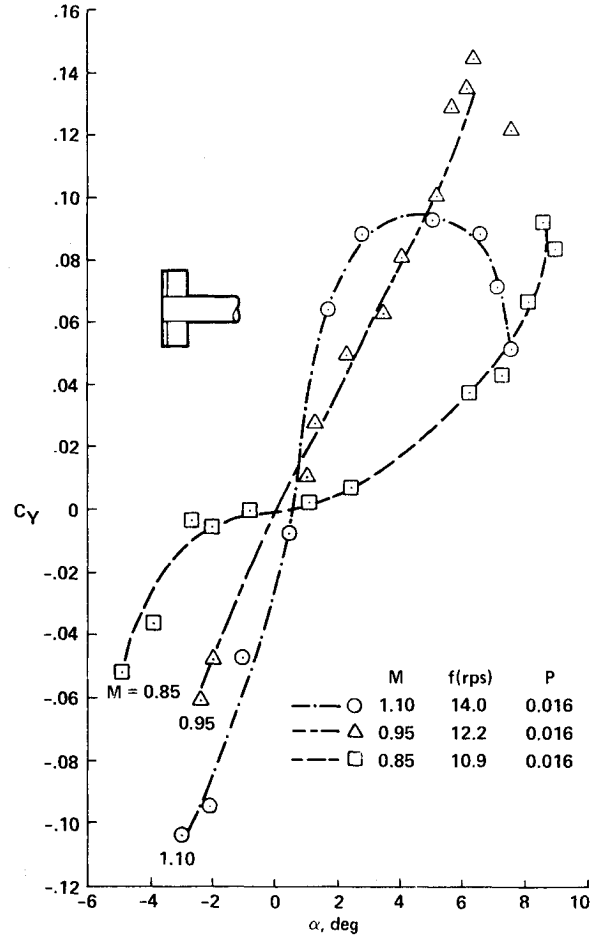

Fig. 7 Side force variation. Full span roll controls, $\delta_e=7$ deg.

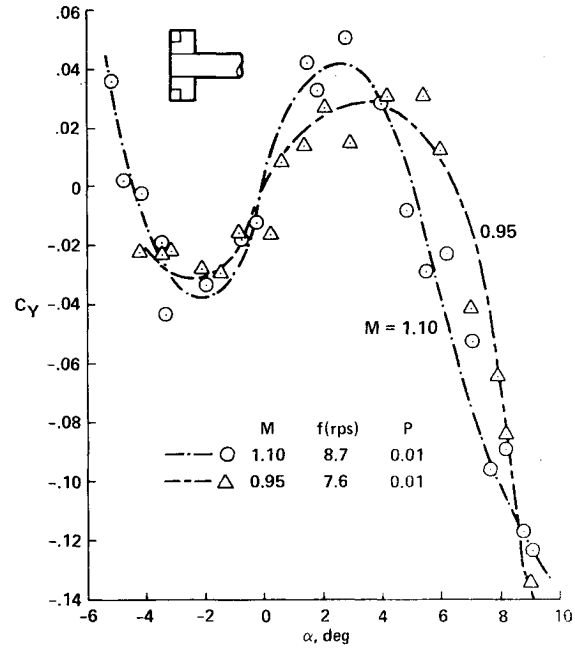

Fig. 8 Side force variation. Outboard roll controls, $\delta_e=7$ deg.

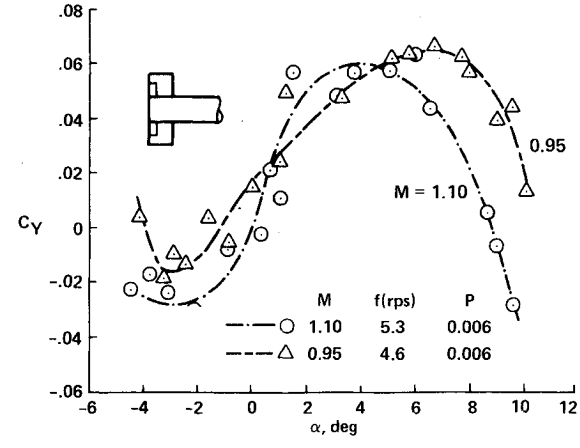

Fig. 9 Side force variation. Inboard roll controls, $\delta_e=7$ deg.

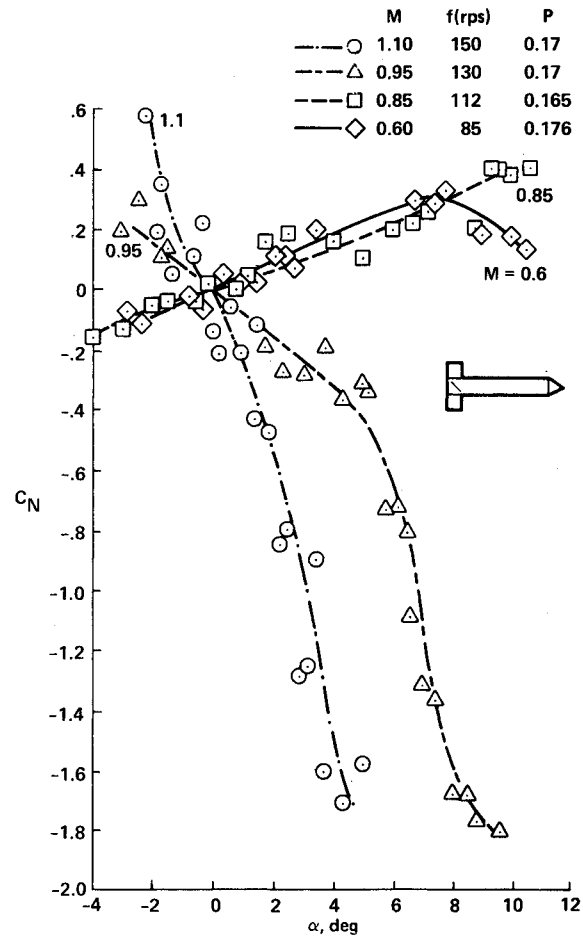

Fig. 10 Yaw moment variation. Full fins deflected, $\delta_e = 7$ deg.

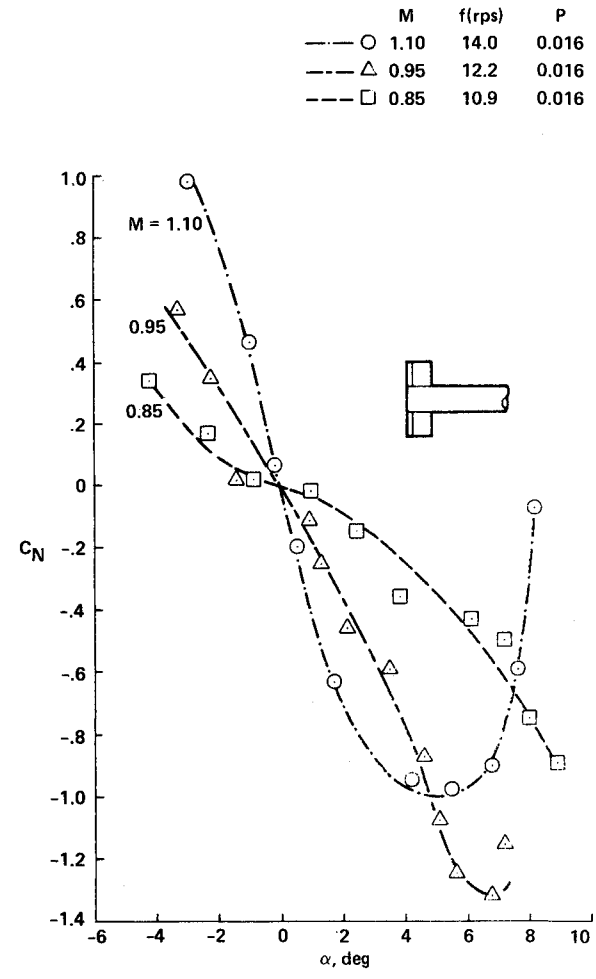

Fig. 12 Yaw moment variation. Full span roll controls, $\delta_e = 7$ deg.

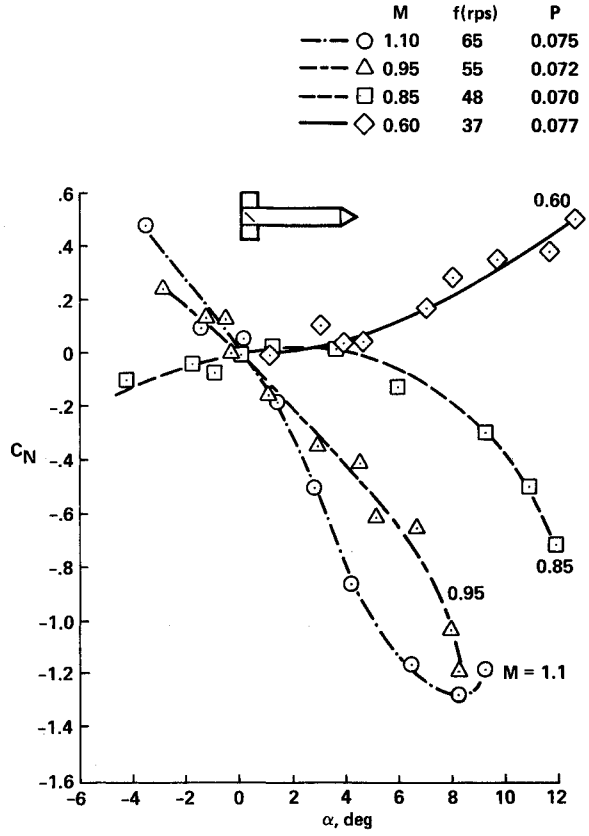

Fig. 11 Yaw moment variation. Full fins deflected, $\delta_e = 3$ deg.

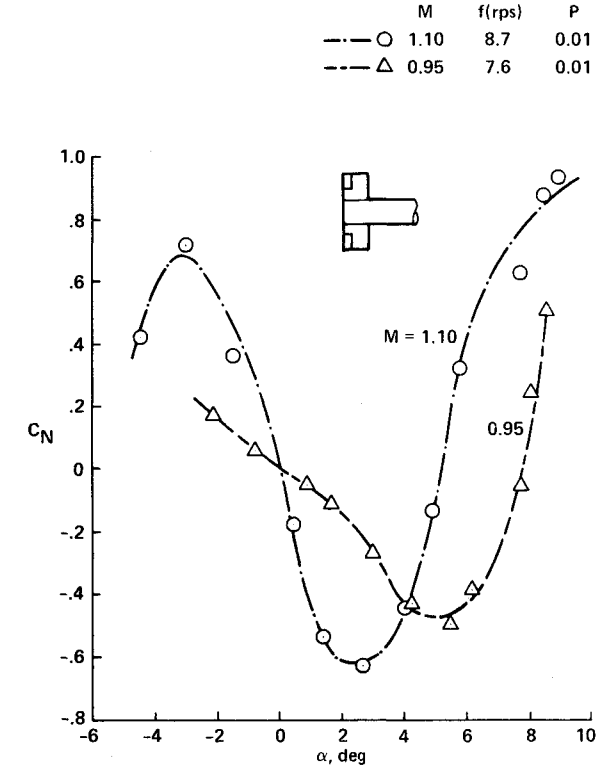

Fig. 13 Yaw moment variation. Outboard roll controls, $\delta_e = 7$ deg.

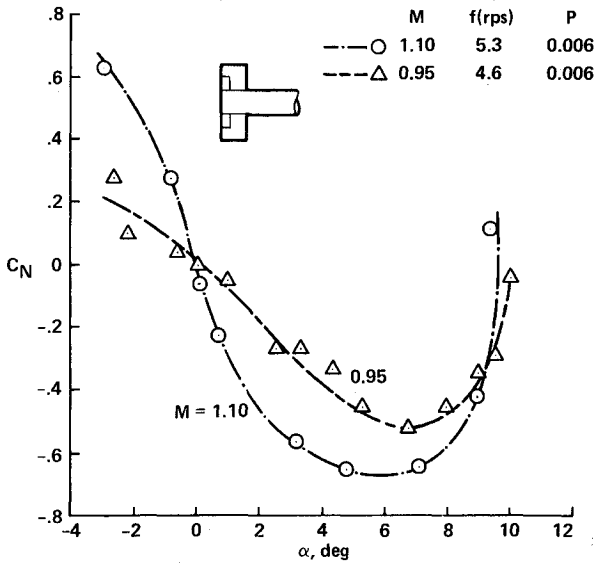

Fig. 14 Yaw moment variation. Inboard roll controls, $\delta_e = 7$ deg.

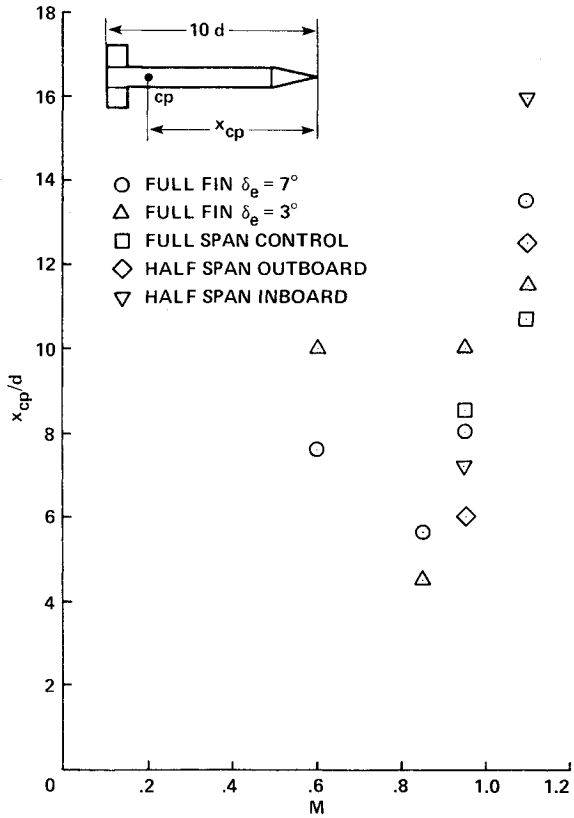

Fig. 15 Center of pressure variation.

(somewhere in the vicinity of $M = 0.8$) at which the center of pressure is at its most forward position. The position of the Magnus center of pressure differs for each configuration. This may be caused by the different cant angle of the fins or different roll controls. It also may be the result of the different reduced roll rates although it was found[22] that for a nonfinned body, the position of the Magnus center of pressure did not vary with the spin rate.

Conclusions

The Magnus force and moment data, measured at transonic speeds on a basic finner model spinning at several spin rates, show that for all reduced spin rates in the present test range, there exists a critical Mach number above which the Magnus force and moment reverse their signs and oppose their classic directions. The critical Mach number of the sign reversal increases when the reduced spin rate is increased. At very low reduced spin rates, the reverse (nonclassic) Magnus loads are found at low angles of attack only, and they change back to their classic sense when the angle of attack is increased. These effects cannot be explained by the known Magnus-force inducing mechanisms either on an axisymmetric body or on a finned configuration, so an additional mechanism was proposed. This mechanism included the interaction of the asymmetric pair of vortices shed from the body and deflected by the spinning-fins induced circulation with the leeward fin. Mach-number, spin-rate, and angle-of-attack effects on this mechanism were qualitatively analyzed.

Another set of conclusions concerns the spin rate variation of the Magnus phenomenon and its center of pressure and should be of interest to finned-configuration designers. The spin rate and the location of the Magnus center of pressure of the basic spinner are independent of the angle of attack. The reduced spin rate is independent also of the Mach number (within the range tested here). The Magnus center of pressure, on the other hand, varies with Mach number. This variation, which differs for the several configurations and could therefore depend also on the spin rate, seems to indicate some critical Mach number where the center of pressure is at its most forward position. The criticial Mach number could be the one at which the Magnus force direction switches.

Additional data are required to substantiate the interaction mechanism proposed here and some of the conclusions.

Acknowledgments

At the time of preparation of this paper the senior author was a National Research Council Senior Research Associate at NASA-Ames Research Center. He wishes to thank the NRC and NASA for their support. Part of the material presented here is based on the second author's Master's research thesis.

References

[1]Cohen, C.J., Clare, T.A., and Stevens, F.L., "Analysis of the Nonlinear Rolling Motion of Finned Missiles," AIAA Paper 72-980, Sept. 1972.

[2]Nicolaides, J.D., Ingram, C.W., and Tarkowski, D.D., "Nonlinear Aerodynamic Characteristics of Sounding Rockets," AIAA Paper 70-1383, Dec. 1970.

[3]Murphy, C.H., "Effect of Roll on Dynamic Instability of Symmetric Missiles," *Journal of the Aeronautical Sciences,* Vol. 21, Sept. 1959, pp. 643-644.

[4]Murphy, C.H., "Free Flight Motion of Symmetric Missiles," Ballistic Research Laboratories, Aberdeen Proving Ground, MD, BRL Rept. 1216, July 1963.

[5]Nicolaides, J.D., "On the Free Flight Motion of Missiles Having Slight Configurational Asymmetries," Ballistic Research Laboratories, Aberdeen Proving Ground, MD, BRL Rept. 858, June 1953.

[6]Vaughn, H.R., "A Detailed Development of the Tricyclic Theory," Sandia Laboratories, Albuquerque, NM, Rept. SC-M-67-2933, Feb. 1968.

[7]Platou, A.S., "Magnus Characteristics of Finned and Nonfinned Projectiles," *AIAA Journal,* Vol. 3, Jan. 1965, pp. 83-90.

[8]Nicolaides, J.D., Eikenberry, R.S., Ingram, C.W., and Clare, T.A., "Flight Dynamics of the Basic Finner Missile," AFATL, Eglin Air Force Base, FL, Rept. No. TR-68-82, July 1968.

[9]Martin, H.R., "An Analytic Method for Predicting the Magnus Force and Moment on Spinning Projectiles," Ballistic Research Laboratory, Aberdeen, MD, Rept. 870, June 1955.

[10]Power, H.L. and Iversen, J.D., "Magnus Effect on Spinning Bodies of Revolution," *AIAA Journal,* Vol. 11, April 1973, pp. 417-418.

[11]Fletcher, C.A.J., "Negative Magnus Force in the Critical Reynolds Number Regime," *Journal of Aircraft,* Vol. 9, Dec. 1972, pp. 826-834.

[12]Benton, E.R., "Supersonic Magnus Effect on a Finned Missile," *AIAA Journal,* Vol. 2, Jan. 1964, pp. 153-155.

[13]Uselton, J.C. and Carman, J.B., "A Study of the Magnus Effects on a Sounding Rocket at Supersonic Speeds," *Journal of Spacecraft and Rockets,* Vol. 8, Jan. 1971, pp. 28-34.

[14]Rosenwasser, I., "Magnus Forces on Axisymmetric Fin Stabilized Rolling Bodies," M.Sc. Thesis, Technion—Israel Institute of Technology, Haifa, Israel, Oct. 1977.

[15]Benton, E.R., "Wing-Tail Interference as a Cause of "Magnus" Effects on a Finned Missile," *Journal of the Aerospace Sciences,* Vol. 29, Nov. 1962, pp. 1358-1367.

[16]Rosenwasser, I. and Seginer, A., "The Measurement of Magnus Forces on Spinning Models," *Proceedings of 23rd Israel Annual Conference on Aviation and Astronautics,* Feb. 1981, pp. 81-88.

[17]Seginer, A. and Ringel, M., "Magnus Effects at High Angles of Attack and Critical Reynolds Numbers," AIAA Paper 83-2145, July 1983.

[18]Regan, F.J. and Falusi, M.E., "The Static and Magnus Characteristics of the M823 Research Store Equipped with Fixed and Freely Spinning Stabilizers," Naval Ordnance Laboratory, White Oak, Silver Spring, MD, NOLTR 72-291, Dec. 1972.

[19]Regan, F.J., "Magnus Measurements on a Freely Spinning Stabilizer," AIAA Paper 70-559, May 1970.

[20]Jacobson, I.D. and Yaggy, P.F., "Magnus Characteristics of Arbitrary Rotating Bodies," AGARDograph 171, Nov. 1973.

[21]Zehentner, R.J., Nelson, R.C., and Mueller, T.J., "A Visual Study of the Influence of Nose Bluntness on the Boundary Layer Characteristics of a Spinning Axisymmetric Body," AIAA Paper 81-1901, Aug. 1981.

[22]Birtwell, E.P., Coffin, J.B., Covert, E.E., and Haldeman, W.C., "Reverse Magnus Force on a Magnetically Suspended Ogive Cylinder at Subsonic Speeds," *AIAA Journal,* Vol. 16, Feb. 1978, pp. 111-116.

[23]Platou, A.S., "Wing-Tunnel Magnus Testing of a Canted Fin or Self-Rotating Configuration," *AIAA Journal,* Vol. 10, July 1972, pp. 965-967.

From the AIAA Progress in Astronautics and Aeronautics Series...

ENTRY VEHICLE HEATING AND THERMAL PROTECTION SYSTEMS: SPACE SHUTTLE, SOLAR STARPROBE, JUPITER GALILEO PROBE—v. 85

SPACECRAFT THERMAL CONTROL, DESIGN, AND OPERATION—v. 86

Edited by Paul E. Bauer, McDonnell Douglas Astronautics Company and Howard E. Collicott, The Boeing Company

The thermal management of a spacecraft or high-speed atmospheric entry vehicle—including communications satellites, planetary probes, high-speed aircraft, etc.—within the tight limits of volume and weight allowed in such vehicles, calls for advanced knowledge of heat transfer under unusual conditions and for clever design solutions from a thermal standpoint. These requirements drive the development engineer ever more deeply into areas of physical science not ordinarily considered a part of conventional heat-transfer engineering. This emphasis on physical science has given rise to the name, thermophysics, to describe this engineering field. Included in the two volumes are such topics as thermal radiation from various kinds of surfaces, conduction of heat in complex materials, heating due to high-speed compressible boundary layers, the detailed behavior of solid contact interfaces from a heat-transfer standpoint, and many other unconventional topics. These volumes are recommended not only to the practicing heat-transfer engineer but to the physical scientist who might be concerned with the basic properties of gases and materials.

Volume 85—Published in 1983, 556 pp., 6×9, illus., $35.00 Mem., $55.00 List
Volume 86—Published in 1983, 345 pp., 6×9, illus., $35.00 Mem., $55.00 List

TO ORDER WRITE: Publications Order Dept., AIAA, 1633 Broadway, New York, N.Y. 10019